Propagation Dynamics of Intense Femtosecond Pulses: Multiple Splittings, Coalescence, and Continuum Generation

Alex A. Zozulya
Department of Physics, WPI, 100 Institute Road, Worcester, Massachusetts 01609-2280

Scott A. Diddams, Amelia G. Van Engen, and Tracy S. Clement*
JILA, University of Colorado and National Institute of Standards and Technology, Boulder, Colorado 80309-0440
(Received 12 August 1998)

We present a scenario of $(3 + 1)$-dimensional spatiotemporal dynamics of femtosecond laser pulses in a nonlinear media with normal dispersion. The sequence of events at progressively higher powers can be characterized as single splitting, multiple splitting, and coalescence. Self-focusing and splitting events are in general spatially separated. Experimental data confirm the above scenario, with measurements at the highest powers corresponding to the regime of continuum generation. [S0031-9007(99)08469-0]

PACS numbers: 42.65.Re, 42.65.Jx

Propagation of electromagnetic pulses is of fundamental importance in pure and applied science, and the recent development of sources of intense femtosecond laser pulses (duration $\leq$100 fs) has added many interesting twists to this long-standing problem. The broad spectral bandwidths, high peak powers, and $(3 + 1)$-dimensional nature of these fields give rise to complex linear and nonlinear effects that have posed significant challenges to researchers. Interesting effects recently seen with high power femtosecond pulses propagating in solids, gases, and liquids include temporal breakup of the pulse [1–3] and extreme spectral broadening—commonly called continuum generation [4–6]. To a large extent, these phenomena rely on the basic process of self-focusing, which is due to an intensity-dependent index of refraction in the propagation medium. It is equally true, however, that these phenomena exist solely because physical mechanisms other than self-focusing are also involved. Were this not the case, one would predict the field to collapse to a spatial singularity after a finite propagation distance in the medium. Because of the associated broad spectral bandwidth, material dispersion typically plays an important role in the propagation of ultrashort pulses. Both self-focusing and material dispersion are accounted for in the formalism of the $(3 + 1)$-dimensional nonlinear Schrödinger (NLS) equation, where it has been shown that for moderate powers normal group velocity dispersion acts to arrest catastrophic spatial collapse with the result of temporal splitting of the input pulse into two [1,7–10].

Spatiotemporal propagation dynamics of ultrashort pulses at slightly higher powers in the framework of the NLS have been the subject of theoretical analysis and varying conjectures [11,12]. One hypothesis is that after the first splitting each of the two newly split pulses may in turn undergo a secondary splitting. Since the NLS theory could not provide definite confirmation of this hypothesis, the dynamics beyond the first splitting have become a topic of active experimental research. Observations of multiple splittings, reported first in Ref. [2] and later in Ref. [3], indicate that reality is sufficiently different from predictions of the idealized NLS model. Sharp temporal features, small beam diameters, and broad bandwidths require that space-time coupling, nonlinear shock, higher-order dispersion, and ionization effects be included in the theoretical analysis aimed at quantitative comparison with experiments [13–21]. The importance of these higher-order terms has become clearer with the use of the newly developed experimental technique of frequency-resolved optical gating (FROG) [22]. The FROG measurement provides both the amplitude and the phase of the pulse and thereby enables quantitative comparison of theory and experiment.

Based on new experimental results, in this Letter we offer a detailed scenario of the spatiotemporal evolution of femtosecond pulses in bulk media with normal group velocity dispersion. We present stages of single and multiple temporal splitting and show that the beam does not undergo further splitting but instead coalesces at still higher powers. Our data also demonstrate that the spatial position z of splitting events is intensity dependent and generally differs from the position of maximum focusing (z is measured along the propagation direction, with $z = 0$ at the entrance of the medium). Experimental observations are in good agreement with the theoretical analysis at all values of the input power, including the regime where continuum generation is observed.

The evolution of the complex envelope $E(\vec{r}, z, t)$ of the field $\mathcal{E}(\vec{r}, z, t) = E(\vec{r}, z, t)\exp(ikz - i\omega_0 t)$ can be modeled with the following modified NLS equation [15–19]:

$$i\frac{\partial}{\partial z}E + \left(1 - i\epsilon_\omega\frac{\partial}{\partial t}\right)\nabla^2 E - \frac{\partial^2}{\partial t^2}E - i\epsilon_3\frac{\partial^3}{\partial t^3}E + \left(1 + i\epsilon_\omega\frac{\partial}{\partial t}\right)g(|E|^2)E = 0. \quad (1)$$

 0031-9007/99/82(7)/1430(4)$15.00

In Eq. (1), the transverse Laplacian ∇^2 accounts for diffraction, while the second and third time derivatives describe group velocity and third order dispersion. The temporal, longitudinal, and transverse coordinates are normalized to the characteristic pulse duration τ, the dispersion length $l_D = 2\tau^2/|k''|$, and the characteristic transverse length $l_\perp = \sqrt{l_D/2k}$, respectively. In addition, $\epsilon_3 = k'''/(3k''\tau)$, and $k = 2\pi n/\lambda$, with n being the linear index of refraction at the central wavelength λ. The dispersion coefficients k'' and k''' are the second and third derivatives of k with respect to frequency, evaluated at the central frequency ω_0. Space-time focusing [14] and nonlinear shock [13] are described by the terms proportional to $\epsilon_\omega = 1/\omega_0\tau$. These terms arise in a self-consistent derivation of Eq. (1) [16,17], and they act together to shift energy towards the trailing edge of the pulse [14,18,19]. Because of the short duration of the pulse, it is important to account for both instantaneous and time-delayed Raman nonlinearities [21,23], such that

$$g(|E|^2) = \frac{2\pi n_2 l_D}{\lambda}\left[(1-\alpha)\,|E(t)|^2 + \alpha\int_{-\infty}^{t} d\tau\, f(t-\tau)\,|E(\tau)|^2\right],$$
$$f(t) = \frac{1+(\omega_r\tau_r)^2}{\omega_r\tau_r^2}\exp(-t/\tau_r)\sin(\omega_r t)\,. \tag{2}$$

In Eq. (2), n_2 is the nonlinear index of refraction, and α denotes the fractional amount of the nonlinearity due to the Raman effect.

Analysis of Eq. (1) shows that typical evolution of an ultrashort pulse consists of a single spatial self-focusing event (at $z = z_f$) followed by irreversible spatial and temporal divergence. The distance z_f is a function of the input power and is the position of the maximum intensity of the field. At relatively low powers a Gaussian-like pulse maintains its spatiotemporal structure. Higher input powers result in a temporal splitting of the pulse into two pulses at $z = z_s$. The temporal splitting and the self-focusing are initially spatially separated, such that $z_s > z_f$, but as the input power is increased, z_s decreases towards z_f. A further increase in the power brings about multiple temporal splitting of the pulse that again happens first at $z > z_f$ and moves towards z_f as the input power is increased. Finally, at still higher powers, the pulse develops a multipeaked structure near the position of maximum focusing, but at $z \gg z_f$ the field coalesces into a broad single pulse. The complete sequence of events at progressively higher powers can be characterized as single splitting, multiple splitting, and coalescence.

Our experiments employ the output of a Ti:sapphire amplified laser system, which is spatially filtered and focused to an intensity full width at half maximum (FWHM) of 70 μm at the entrance face of a 3-cm-thick piece of fused silica. Temporally, the incident field is near bandwidth limited, with an intensity duration of 80–90 fs (FWHM, measured for each experiment). The peak power P is varied between 2 and 8 MW. After propagation in the fused silica, the entire field is allowed to diffract in air over 1.5 m. At this point an aperture of $\sim$1 mm in diameter selects the on-axis portion of the field for characterization by the second-harmonic FROG apparatus [3].

In the theoretical analysis we use parameters corresponding to our experimental setup and the material properties of fused silica in the normal dispersion regime: $\lambda = 800$ nm, $n = 1.45$, $n_2 = 2.5 \times 10^{-16}$ GW/cm^2, $k'' = 360$ fs^2/cm, and $k''' = 275$ fs^3/cm. For the Raman response we use $\alpha = 0.15$, $\tau_r = 50$ fs, and $\omega_r\tau_r = 4.2$ [23]. The initial field is taken to be a hyperbolic secant in time and a Gaussian in space having intensity FWHM of 90 fs and 70 μm, respectively. As in the measurements, the beam waist is located at the entrance face of the sample, which is 3 cm long. Furthermore, the linear propagation of the field from the exit face of the medium (near field) to the measuring device (far field) is included in the model, as discussed in detail below.

The left and center columns of Fig. 1 show the calculated temporal on-axis intensity in the near and far fields, respectively. The right column of Fig. 1 shows the corresponding measured far-field axial intensity profiles at input powers of 3.9, 4.6, and 5.4 MW. For all input powers shown, both the experimental data and the theoretical analysis demonstrate splitting of the pulse in the far field to some degree. However, at the lowest power [Fig. 1(a)] the calculated output of the nonlinear medium remains unsplit. For these data, the position of maximum focusing corresponds to $z_f = 17$ mm. The splitting takes place during free-space propagation of the pulse from the medium to the detecting apparatus. Numerical analysis for the above parameters shows that the splitting would have happened inside the medium if its length was larger than $\sim$65 mm. Figure 1 also demonstrates that with increasing input power, splitting occurs first in the far field and then progresses to the near field. In Fig. 1(e), full splitting is seen in the far field, while splitting is only beginning in the near field. When full splitting does occur in the near field [Fig. 1(c)], the far field is seen to have three distinct pulses on axis [Figs. 1(f) and 1(i)].

Primary splitting of a single-peaked pulse into two pulses has been explained as a result of a modulation instability of a plane wave [7] or in terms of the evolving peak power of the pulse [9]. Without denying these mechanisms, our analysis suggests a complimentary mechanism of splitting based on "geometrical" considerations. In our experiments, the measured axial field includes effects due to the linear propagation from the exit face of the nonlinear medium to the FROG apparatus. The axial far-field

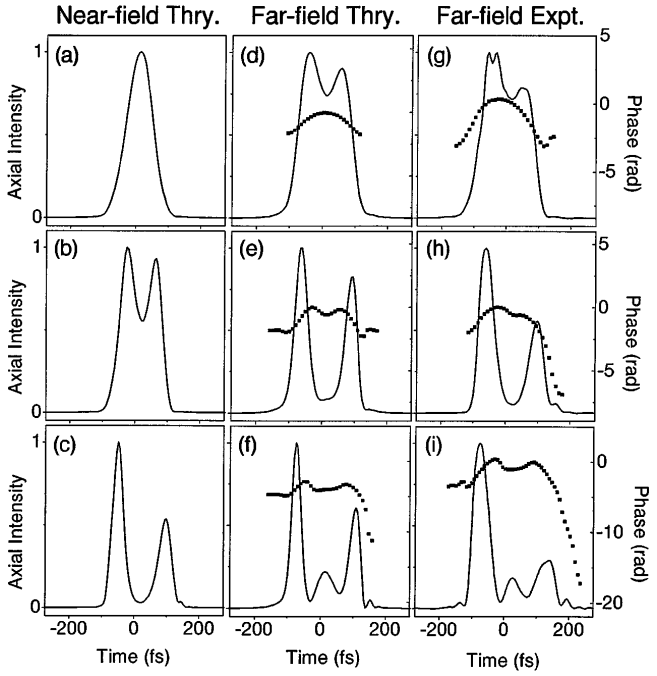

FIG. 1. (a)–(c): Calculated axial intensity at the output face of 3 cm of fused silica. (d)–(f): Calculated axial intensity in the far field for the corresponding fields shown in the left column. (g)–(i): Measured far-field axial intensity for input peak powers of 3.9, 4.6, and 5.4 MW. The points shown in plots (d)–(i) are the calculated and measured phases of the complex field envelope. Powers used in calculations match experimental values to better than 10%.

amplitude can be approximated by the integral over the near-field spatial cross section at the corresponding time: $a(0,\infty,t) \propto \int dr' r' a(r',0,t)$. This result shows that a maximum in the on-axis field can come from either a cross section with the largest values of the field or a cross section with possibly smaller values of the field, but nearly constant phase. This second possibility is quite generally created in a normally dispersive nonlinear medium when the pulse undergoes a focusing event and then diverges without undergoing any immediate splitting. As a simple example, consider a slightly diverging Gaussian pulse with wave-front radius of curvature equal to f. After propagating through a nonlinear medium, this field acquires a nonlinear phase shift such that its amplitude can be written as $E(r,t) = \exp(-r^2 - t^2)\exp[ir^2/f + ilI(r,t)]$, where $I = |E(r,t)|^2 = I_{\max}\exp(-2r^2 - 2t^2)$ and l is the length of the medium. The phase distribution of this field is shown in Fig. 2. Integration over the temporal center of the pulse (line *A*) involves largest values of the amplitude but also rapid changes of the phase. Integration over cross sections *B* and *C* involves smaller values of the amplitude but nearly constant phase. Contributions to the on-axis pulse amplitude in the far field from *B* and *C* will dominate over that from *A*, resulting in the temporal splitting of the pulse into two pulses, provided the nonlinearity is high enough.

At the highest intensities used in our experiments, the three pulses seen in Fig. 1(i) coalesce toward a single broad pulse. This process is shown in Fig. 3, where we plot the measured and calculated far-field axial intensity. Figures 3(a) and 3(b) show the experimental results for $P = 6.8$ and 7.4 MW, respectively. The corresponding calculations are shown in Figs. 3(c) and 3(d), with the input powers matching those of the experiment to within 15%. As can be seen, with increasing power the central peak grows and merges with the leading and trailing peaks. Although the near-field axial intensity contains multiple maxima, distinct multiple pulses similar to those of Fig. 1(i) are not seen in the near-field calculations for the range of parameters investigated here. This is significant and implies that the physical processes responsible for the initial splitting of the input do not necessarily result in the multiple splittings with a simple increase of the input power. When we do observe multiple splittings in the far field, we see that it is more accurately described by constructive buildup of a previously void region of the axial field [see Figs. 1(h) and 1(i)].

Figure 4 shows the measured and calculated spectra for the fields shown in Figs. 3(b) and 3(d). The long tails extending towards both higher and lower wavelengths are evidence of continuum generation, and blue light was clearly visible by the eye for this measurement. A recent work by Brodeur and Chin [6] associates the extensive blue spectrum with multiphoton excitation and the resulting negative change of the index of refraction. The absence of such mechanisms in the analysis of Eq. (1) is a probable reason for the difference on the short-wavelength side between the spectra of Fig. 4.

The coalescence of the pulse at high intensities may also qualitatively explain recent results of Ranka *et al.* [2], who made autocorrelation measurements of multiple pulse splitting in a regime similar to that discussed here. They

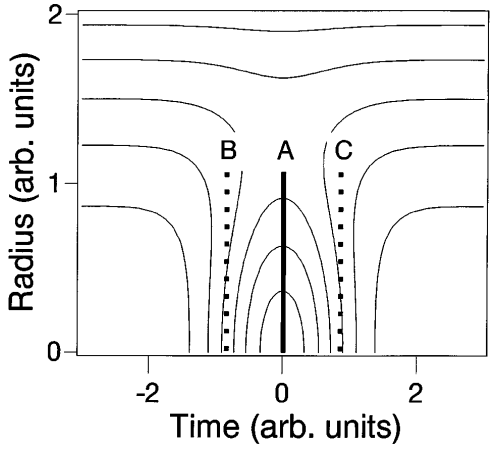

FIG. 2. Contour plot of the phase of a slightly diverging self-focused pulse as given in the text. Cross sections at *B* and *C* have larger contributions in the far field because of the near constancy of the phase.

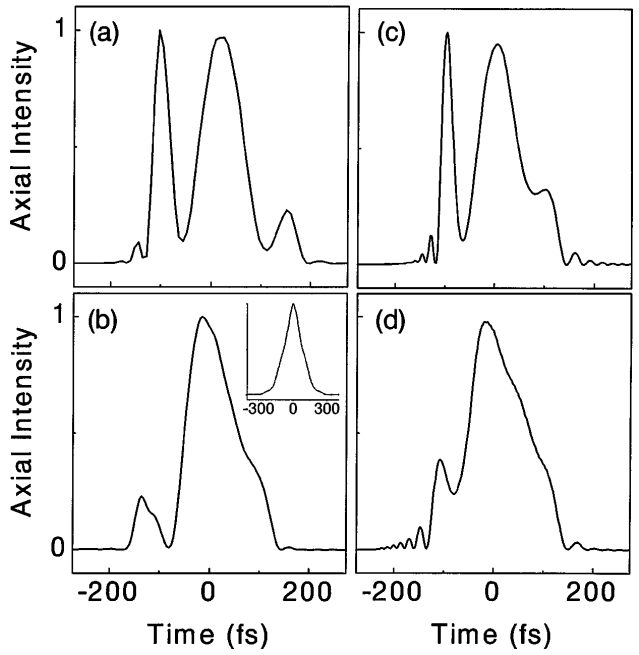

FIG. 3. (a)–(b): Measured axial intensities demonstrating coalescence for input powers of 6.8 and 7.4 MW. (c)–(d): Calculated axial intensities. The inset of plot (b) is the simultaneously measured intensity autocorrelation.

observed multiple pulse splitting in a 1.3 cm piece of a BK-7 glass but were not able to observe multiple splittings for the same powers in a 2.5 cm sample. According to our interpretation, at a given power multiple splitting may be observed in a relatively small length of the medium. However, for a longer medium, multiple pulses coalesce by the time they reach the detector, resulting in an autocorrelation lacking multiple peaks [see inset of Fig. 3(b)].

The results presented here illustrate a new scenario of the complex dynamics involved in the nonlinear focusing and propagation of intense femtosecond pulses. We have shown that such a pulse first undergoes a single splitting, then multiple splittings, and finally coalescence. These results should be valuable for applications involving intense femtosecond pulses, including spatiotemporal tailoring for propagation in other nonlinear media.

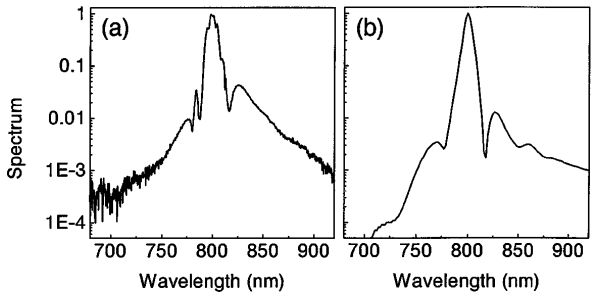

FIG. 4. (a) Measured axial spectrum for the field shown in Fig. 3(b). (b) Calculated axial spectrum for the field of Fig. 3(d).

This research was supported in part by the National Science Foundation and the National Institute of Standards and Technology.

*Current address: Optoeletronics Division, National Institute of Standards and Technology, 325 Broadway, Boulder, CO 80303.

[1] D. Strickland and P. B. Corkum, J. Opt. Soc. Am. B **11**, 492 (1994).
[2] J. K. Ranka, R. W. Schirmer, and A. L. Gaeta, Phys. Rev. Lett. **77**, 3783 (1996).
[3] S. A. Diddams, H. K. Eaton, A. A. Zozulya, and T. S. Clement, Opt. Lett. **23**, 379 (1998).
[4] R. L. Fork, C. V. Shank, C. Hirlimann, and R. Yen, Opt. Lett. **8**, 1 (1983).
[5] P. B. Corkum, C. Rolland, and T. Srinivasan-Rao, Phys. Rev. Lett. **57**, 2268 (1986).
[6] A. Brodeur and S. L. Chin, Phys. Rev. Lett. **80**, 4406 (1998).
[7] N. A. Zharova *et al.*, JETP Lett. **44**, 13 (1986).
[8] P. Chernev and V. Petrov, Opt. Lett. **17**, 172 (1992).
[9] J. E. Rothenberg, Opt. Lett. **17**, 583 (1992).
[10] G. G. Luther, J. V. Moloney, A. C. Newell, and E. M. Wright, Opt. Lett. **19**, 862 (1994).
[11] G. Fibich, V. M. Malkin, and G. C. Papanicolaou, Phys. Rev. A **52**, 4218 (1995).
[12] L. Bergé and J. J. Rasmussen, Phys. Rev. A **53**, 4476 (1996).
[13] F. DeMartini, C. H. Townes, T. K. Gustafson, and P. L. Kelley, Phys. Rev. **164**, 312 (1967).
[14] J. Rothenberg, Opt. Lett. **17**, 1340 (1992).
[15] J. T. Manassah and B. Gross, Laser Phys. **6**, 563 (1996).
[16] G. Fibich and G. C. Papanicolaou, Opt. Lett. **22**, 1379 (1997).
[17] T. Brabec and F. Krausz, Phys. Rev. Lett. **78**, 3282 (1997).
[18] J. K. Ranka and A. L. Gaeta, Opt. Lett. **23**, 534 (1998).
[19] A. A. Zozulya, S. A. Diddams, and T. S. Clement, Phys. Rev. A **58**, 3303 (1998).
[20] Q. Feng *et al.*, IEEE J. Quantum Electron. **33**, 127 (1997).
[21] M. Mlejnek, E. M. Wright, and J. V. Moloney, Opt. Lett. **23**, 382 (1998).
[22] R. Trebino *et al.*, Rev. Sci. Instrum. **68**, 3277 (1997).
[23] R. Hellwarth, J. Cherlow, and T.-T. Yang, Phys. Rev. B **11**, 964 (1975); R. H. Stolen, J. P. Gordon, W. J. Tomlinson, and H. A. Haus, J. Opt. Soc. Am. B **6**, 1159 (1989); R. H. Stolen and W. J. Tomlinson, J. Opt. Soc. Am. B **9**, 565 (1992).